Title
Alternating Laser Excitation for Solution-Based Single-Molecule FRET.

Journal
Cold Spring Harbor Protocols, 2015(11)

ISSN
1940-3402

Authors
Kapanidis, Achillefs
Majumdar, Devdoot
Heilemann, Mike
et al.

Publication Date
2015-11-01

DOI
10.1101/pdb.top086405

Peer reviewed

Topic Introduction

Alternating Laser Excitation for Solution-Based Single-Molecule FRET

Achillefs Kapanidis, Devdoot Majumdar, Mike Heilemann, Eyal Nir, and Shimon Weiss

Single-molecule fluorescence resonance energy transfer (smFRET) has been widely applied to the study of fluorescently labeled biomolecules on surfaces and in solution. Sorting single molecules based on fluorescent dye stoichiometry provides one with further layers of information and also enables "filtering" of unwanted molecules from the analysis. We accomplish this sorting by using alternating laser excitation (ALEX) in combination with smFRET measurements; here we describe the implementation of these methodologies for the study of biomolecules in solution.

INTRODUCTION

The development of single-molecule FRET (smFRET) (Ha et al. 1996) introduced a powerful technique to probe conformational states of single biomolecules. Widespread adoption and application of smFRET in a short period of time by the biological community has helped establish the method as a tool to characterize conformational dynamics (in the 1- to 10-nm range) of single molecules in very dilute solutions or immobilized on surfaces. Often, this approach has unearthed new and important information about the mechanisms underpinning the function of a broad range of biological machines (Ha 2001, 2004).

Typically, a solution-based smFRET experiment involves the detection of photons from one donor and a nearby acceptor fluorophore, and this information is used to arrive at a ratio for energy transfer (FRET) that reports on the distance between the donor and acceptor dyes. However, if the dyes are far apart, it is impossible to distinguish between a solitary donor (without nearby acceptor) and a donor with a distant companion acceptor (well beyond the range of FRET, ~1–10 nm for common dyes).

To remedy this problem, we developed alternating laser excitation (ALEX) (Kapanidis et al. 2004, 2005a; Laurence et al. 2005; Lee et al. 2005; Nir et al. 2006), which provides additional and direct information on the presence and the state of both donor and acceptor fluorophores in the molecules of interest. The additional information leads to multidimensional histograms of FRET and fluorophore stoichiometry, which, in turn, report on biomolecular structure and stoichiometry, respectively. Initial applications of ALEX focused on studies of gene transcription (Kapanidis et al. 2005b, 2006; Margeat et al. 2006) and protein folding (Jager et al. 2005, 2006; Laurence et al. 2005; Hamadani and Weiss 2008). As with conventional smFRET, ALEX is compatible with studies of both diffusing and immobilized molecules. Diffusing molecules can be studied in solutions, gels, or even porous materials; immobilized molecules can be studied using confocal microscopy and scanning, or total internal reflection (TIR) wide-field microscopy (Margeat et al. 2006).

This introduction describes methods based on ALEX of single molecules in solution; advice is given for building instrumentation for basic analysis of diffusing with general instructions for data analysis.

Adapted from *Imaging: A Laboratory Manual* (ed. Yuste). CSHL Press, Cold Spring Harbor, NY, USA, 2011.

Cite this introduction as *Cold Spring Harb Protoc*; doi:10.1101/pdb.top086405

Detailed information is presented on preparing standards for alignment and evaluation of the sensitivity of the setup in **Assembling the µs-ALEX Setup** (Kapanidis et al. 2015a), **Aligning the µs-ALEX Setup** (Kapanidis et al. 2015b), and **Sample Preparation and Data Acquisition for µs-ALEX** (Kapanidis et al. 2015c).

THEORY: FRET AND ALEX RATIOS

Single-excitation FRET measures photon counts $f_{D_{ex}}^{D_{em}}$ and $f_{D_{ex}}^{A_{em}}$, where f_X^Y is the photon count for a single molecule on excitation at wavelength X (where D_{ex} is the wavelength of substantial excitation of the FRET donor) and detection at wavelength range Y (where D_{em}, A_{em} are wavelengths of substantial emission of FRET donor and acceptor, respectively). ALEX provides one more nonzero photon count, $f_{A_{ex}}^{A_{em}}$, for acceptor emission on direct acceptor excitation (Kapanidis et al. 2004; Lee et al. 2005). These three-photon counts allow calculation of the proximity ratio E_{PR}^{raw} and the relative fluorescence stoichiometry ratio S^{raw}:

$$E_{PR}^{raw} = \frac{f_{D_{ex}}^{A_{em}}}{f_{D_{ex}}^{A_{em}} + f_{D_{ex}}^{D_{em}}},$$

$$S^{raw} = \frac{f_{D_{ex}}}{f_{D_{ex}} + f_{A_{ex}}} = \frac{f_{D_{ex}}^{D_{em}} + f_{D_{ex}}^{A_{em}}}{f_{D_{ex}}^{D_{em}} + f_{D_{ex}}^{A_{em}} + f_{A_{ex}}^{A_{em}}}.$$

This additional information is summarized in two-dimensional histograms (Fig. 1) and allows virtual molecular sorting. Sorting can remove artifacts that complicate FRET (such as the presence of states with inactive FRET donor or acceptor, and the presence of complex fluorophore stoichiomeries) while introducing new entities that can be observed, such as an A-only population, which is helpful for evaluating biomolecular interactions.

The nature and timescale of the biological question to be addressed, along with the required measurement sensitivity, determine the alternation timescale for ALEX. Basic experiments concerning equilibrium views of a biological system (as well as kinetics occurring in the few-minute timescale) can be pursued using laser modulation at the microsecond timescale by what we dub as microsecond-ALEX (µs-ALEX), which provides snapshots of diffusing molecules.

As in smFRET experiments, typical ALEX-based methods require the use of subnanomolar concentrations of labeled molecules to ensure that single molecules can be detected and analyzed. Moreover, fluorescent probes need to be attached to molecules of interest, and assays need to show that the fluorophores do not significantly perturb their function. Finally, fluorophore photobleaching sets a limit on the observation of immobilized molecules, especially in the absence of oxygen scavengers and chemical additives. For information on bioconjugation chemistries and fluorophores repeat that are compatible with single-molecule fluorescence, see Kapanidis and Weiss (2002) and Jager et al. (2005, 2006).

PRACTICE: DESIGN PRINCIPLES FOR smFRET SETUP

Excitation

Using confocal optics, single molecules are detected during transit through the confocal volume, wherein a focused laser beam excites the molecules and from which emitted photons are detected. In the "photon-hungry" regime of single-molecule measurements, the confocal microscope enables measurements with negligible background; the low background can be attributed to the pinhole in the optical path. Whereas most details for microscope construction do not at all deviate from traditional

Cite this introduction as *Cold Spring Harb Protoc;* doi:10.1101/pdb.top086405

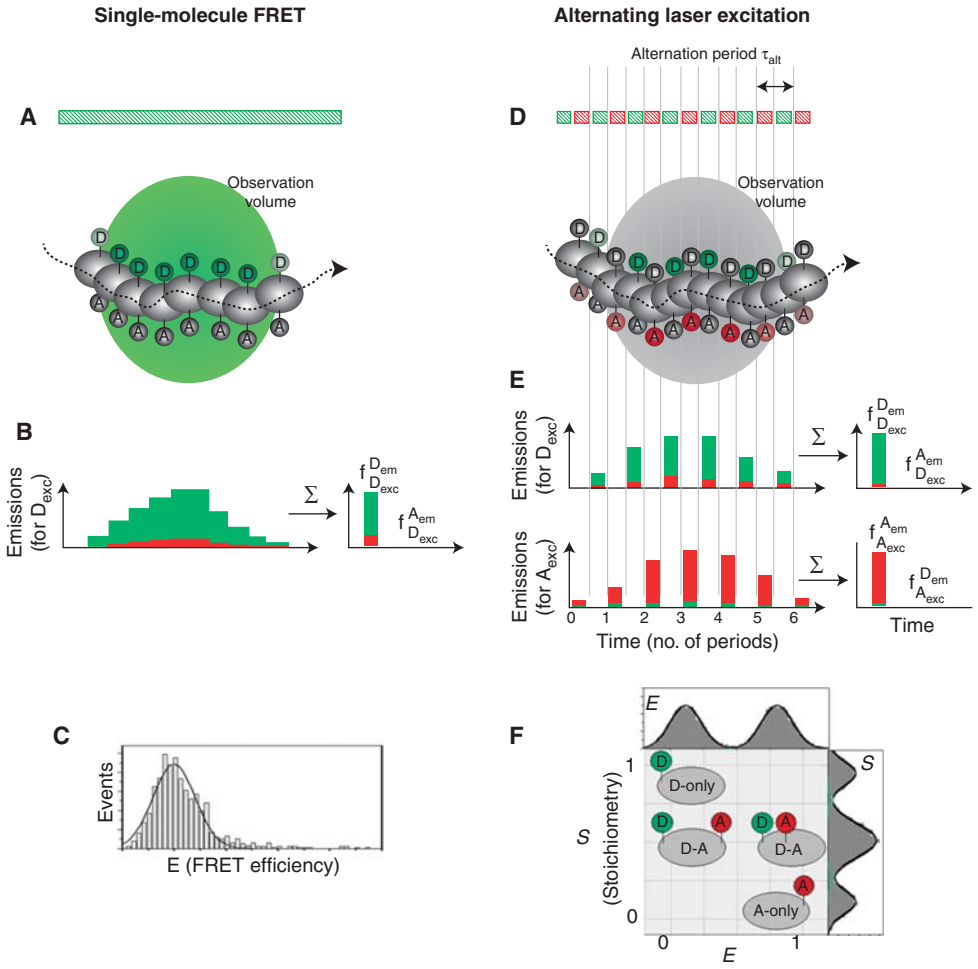

FIGURE 1. Concept of ALEX and comparison with single-excitation single-molecule FRET. (*A–C*) Single-molecule FRET using single-laser excitation; diffusing-molecule example. A fluorescent molecule traverses a focused green-laser beam and emits photons in the donor- and acceptor-emission wavelengths. The photon counts at these two wavelengths are used to generate one-dimensional histograms of FRET efficiency *E*. (*D,E*) Single-molecule FRET using alternating laser excitation. A fluorescent molecule traverses an observation volume illuminated in an alternating fashion using focused green- and red-laser beams. Using the photons emitted in the donor- and acceptor-emission wavelengths for each laser excitation, one can generate a two-dimensional histogram of FRET efficiency *E* and relative fluorophore stoichiometry *S*, enabling molecular sorting (see text for details).

confocal setups (also used for fluorescence correlation spectroscopy or imaging), here we discuss some practical implementation specific to smFRET/ALEX-type microscope setups.

To probe both donor (for FRET) and acceptor (for ALEX) dyes, the laser beam must be "chopped" between alternating periods of donor and acceptor excitation. There are three main ways to modulate the laser excitation, depending on the type of laser (diode, solid state, gas) and general requirements (frequency and rise time, flexibility, cost, ease of use).

Acousto-Optical Modulation

This is easy to align and operate, with frequencies up to 15 MHz and rise times of ~25 nsec (for $PbMnO_4$ as the acousto-optical material). An acousto-optic modulator (AOM) is inexpensive, and operation with all types of linearly polarized continuous wave lasers is possible, thus increasing the flexibility of a setup. Similar to AOMs, acousto-optical tunable filters (AOTFs) can be used, allowing modulation of multiple wavelengths by selective deflection (Nir et al. 2006; Ross et al. 2007).

Direct Modulation

This method is applicable to solid-state lasers; modulation is achieved by direct modulation of the laser power via TTL signals (transistor–transistor logic, which refers to a standardized digital signal), which can achieve high frequencies of up to 100 MHz (for diode lasers) and short rise times (2 nsec). Directly modulated diode lasers represent the most convenient option, as no additional optical components are necessary (see Kong et al. 2007). However, the current cost of these lasers and low power output (often 5–10 mW) remains a major drawback to this approach.

Electro-Optical Modulation

Basic electro-optic modulators (EOMs) can reach frequencies up to ~1 MHz with rise times of ~100 nsec, and thus fulfill the requirements for µs-ALEX; most of the published ALEX work is based on electro-optical modulation. However, this method is rather expensive and requires additional optical elements (quarter-wave plates and half-wave plates) and space.

All modulation devices can easily be addressed through software-controlled TTL or analog signals. All of these options work well for µs-ALEX, as modulation frequencies of 10 kHz–100 kHz are used. However, direct modulation of a laser is, if available, the easiest option.

Emission

Fluorescence light leaving the microscope through the base port is directed toward the detection module (Fig. 2). After the base port of the microscope, a pinhole is placed at the focal point of the microscope lens. (This is the "tube lens." The focal length is available from the manufacturer. Usually, the focal point is close to the base port of the microscope.) The pinhole is mounted onto an *x–y* positioner with micrometer screws, allowing easy removal or repositioning. This is helpful for the first alignment, as the detectors can be aligned without a pinhole. Single-molecule experiments will necessitate use of a 50–150-µm pinhole, depending on background of solution and solution viscosity.

After the pinhole, the light is collimated with another lens and spectrally separated with a single-band dichroic beam splitter. In combination with emission filters in front of the detectors, these elements should match the spectral characteristics of the setup and the fluorophores (i.e., eliminating excitation wavelengths and contributions to background signal by Raman scattering), thereby assuring efficient detection of the selected fluorophores. Point source detectors should be chosen for µs-ALEX applications. These detectors are most often avalanche photodiodes (APDs; also known as

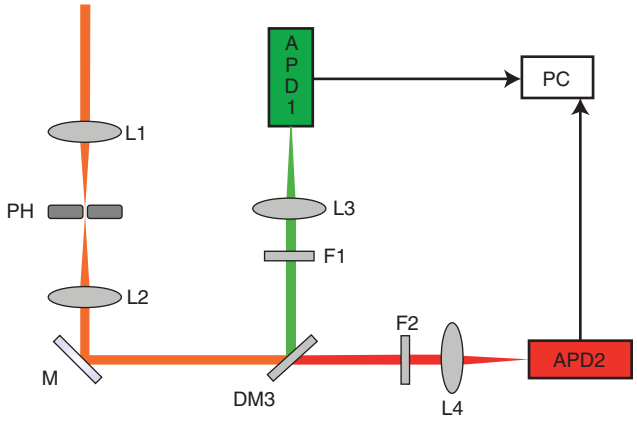

FIGURE 2. Emission module for ALEX. Fluorescence emission collected by the objective and through the DM of the sample holder module is focused with lens L1 onto a pinhole (PH), parallelized by L2, and separated according to wavelength by a dichroic beam splitter DM3 (650 DRLP). Light is directed through filters F1 (585DF70) and F2 (650LP) to select emission spectrum. Lenses L3 and L4 (20-mm focal length) focus onto the active area of the detectors (APD1 and APD2).

Cite this introduction as *Cold Spring Harb Protoc*; doi:10.1101/pdb.top086405

single-photon avalanche diodes or SPADs), showing a low electronic background noise (termed "dark counts," as no photon is actually detected) and high detection efficiency for a single photon. The arrival of a photon on the active area of the detector generates an electric signal, which is sent to a PCI (Peripheral Component Interconnect) board (e.g., PCI-6602, from National Instruments) and is then processed by acquisition software. It is crucial to shield the whole detection module from external light, using a black box (e.g., made of black cardboard) placed around the module.

DATA ANALYSIS

Burst Search

Because single-molecule measurements are performed using ~10–100 pM solutions of fluorescent molecules, the confocal volume is occupied by a fluorescent molecule for <~10% of the time; during the remaining ~90% or more of the time, photons detected are background photons. This background, with intensities of several thousands of photons per second (several kHz), is mostly attributed to Raman scattering of water and buffer molecules, labeled molecules diffusing at the fringe of the confocal spot, and reflections from optics. These contributions are in addition to the APD dark count. During the transit time (~1 msec) of the fluorescent molecule through the confocal volume, a finite number of excitation/emission cycles occur, resulting in a burst of fluorescence photons. This fluorescence burst is the observable result for a single diffusing molecule. When analyzing the stream of photons, one needs to distinguish between background photons and the photons of a burst and to assign the beginning and end of such a burst.

Fixed-Bin Burst Search

A simple way to separate fluorescence from background photons is to use the so-called "Box-Filter" search algorithm. During this search, the photon arrival time record is sectioned into fixed time intervals (bins) (Deniz et al. 1999). Using a photon-count threshold (the minimum number of photons per bin), bins containing fewer photons than the threshold are ignored, whereas bins containing more photons than the threshold are identified and retained for further analysis. Typical search parameters for standard fluorophores are bin durations of 500 μsec and photon-count thresholds of 5–20 photons. This algorithm lacks correlation between fixed bins and stochastically appearing bursts, because a burst (from a single molecule) may be divided into two bins. Moreover, a bin may contain predominantly background photons in addition to the burst of photons. This approach cannot be used efficiently in the dual-channel burst search (see below), because it cannot detect the exact moment in which a donor or acceptor molecule becomes inactive.

Sliding Burst Search

Sliding burst search is an alternative approach introduced by Seidel and coworkers (Eggeling et al. 2001). During this search, a burst is identified if at least L successive photons have at least M neighboring photons within a time window of length T centered on their own arrival time. The first and the last photons satisfying these criteria define the "start" and "stop" photons, respectively. Typical search parameters used are $L = 10–50$, $M = 2–10$, and $T = 100–1000$ μsec. The photons considered in this burst search can be photons detected during donor-excitation periods, acceptor-excitation periods, or all excitation periods ("all-photons" burst search or APBS) (Nir et al. 2006).

ALEX-Based Burst Search

Because the APBS identifies bursts irrespective of the wavelength of laser excitation and fluorescence emission, it may lead to skewed FRET values for molecules that bleach or blink during their transit through the confocal spot. An ALEX-based burst search can eliminate such events; here, the sliding burst search is used separately for (1) photons detected during donor-excitation periods, indicating

the time intervals during which the donor is present and is photoactive, and (2) photons detected during acceptor-excitation periods, indicating the time intervals during which the acceptor is present and is photoactive. During this burst search, photons are considered as part of a burst if their time of arrival overlaps with the time intervals (1) and (2). This ensures identification of bursts containing photons detected during time intervals when both fluorophores are photoactive (thus removing any skew in the FRET distribution). The laser-alternation periods are considerably shorter than the sliding window. We dub this search the dual-channel-burst search (DCBS), where "dual-channel" refers to donor excitation versus acceptor excitation (and not donor emission vs. acceptor emission). Typical search parameters are $L = 5–25$, $M = 2–10$, and $T = 100–1000$ μsec. A subset of DCBS monitors solely the presence and state of the acceptor in diffusing molecules (Kapanidis et al. 2005b).

ALEX-Related Histograms and Factors Affecting Them

After burst search and identification, one can calculate two fluorescence ratios: proximity ratio E^{raw}_{PR} and stoichiometry S^{raw} (see above, Theory: FRET and ALEX Ratios, and below, μs-ALEX: Measuring Accurate FRET Efficiencies) for each burst. In this section, we use the general terms E and S to refer to these two ratios and to corrected versions thereof. For a complete treatment, see below, μs-ALEX: Measuring Accurate FRET Efficiencies, and Lee et al. (2005). The two ratios are then plotted in a 2D histogram, as well as two related 1D histograms (the collapse of the 2D histogram onto the proximity-ratio axis or the stoichiometry axis) (Fig. 3). For better representation, the results are "binned," usually by dividing the entire range of E or S (0.00–1.00) in 50–100 bins. To extract reliable information from the 2D histograms, one needs to understand how the histogram is affected by factors such as statistical fluctuations, molecular dynamics, and experimental artifacts. In part, this is achieved using dual-color burst search (Fig. 3).

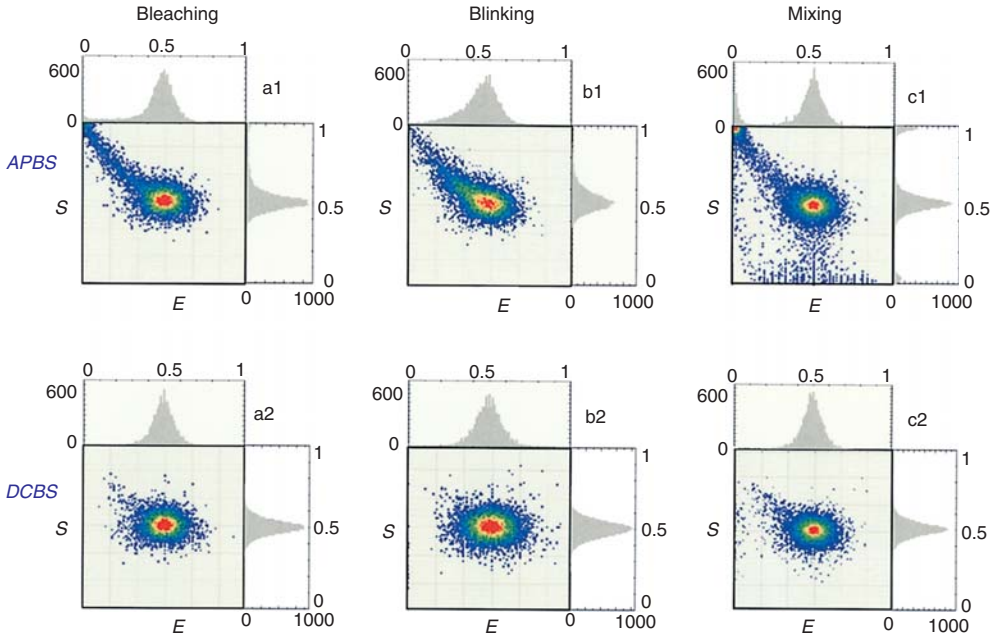

FIGURE 3. Simulated effects of bleaching, blinking, and random coincidence on the 2D *E*–*S* histogram: Comparison of all-photons burst search (APBS; *upper* row) with the dual-channel-burst-search (DCBS; *lower* row). Bleaching (*left*) and blinking (*middle*): In both cases, APBS reveals a trail of bursts connecting a *D*-only population ($E = 0$, $S = 1$) and the population of interest ($E = S = 0.5$). DCBS eliminates such bursts, yielding symmetric, Gaussian-like *E* and *S* distributions. Random coincidence (*right*): APBS reveals a trail of bursts from the *D*–*A* population toward the *D*-only subpopulation and toward the *A*-only subpopulation ($S = 0$). Again, DCBS eliminates most of these bursts, resulting in symmetric, Gaussian-like *E* and *S* distributions (see also Nir et al. 2006).

Cite this introduction as *Cold Spring Harb Protoc*; doi:10.1101/pdb.top086405

Shot Noise

In the absence of artifacts (e.g., fluorophore photophysics), the main factors affecting the shape and width of subpopulations in the efficiency versus stoichiometry, or *E*–*S*, histogram are the donor to acceptor, or *D*–*A*, distance distribution and the shot noise (statistical fluctuation or noise). If the *D*–*A* distance is fixed and identical for all molecules, then the histogram shape and width result from the statistical fluctuation of photon counts around an average. For example, if we assume that *E* is 0.5 and all bursts have 100 photons, then because of statistical noise, the actual number of acceptor photons will vary around 50 (because $E = f_{D_{ex}}^{A_{em}}/(f_{D_{ex}}^{A_{em}} + f_{D_{ex}}^{D_{em}}) = 0.5$ when $f_{D_{ex}}^{A_{em}} = f_{D_{ex}}^{D_{em}} = 50$) but will not always be equal to 50. Because of the stochastic character of the donor and the acceptor emissions, the fluctuation around the average can be described by a binomial law and depends on the size of a burst (i.e., the sum of donor and acceptor photons in a burst) and the probability that a photon in a burst is an acceptor photon. In the absence of background and cross talk photons (or after accounting for such contributions), this latter probability is equal to the *E* value (Lee et al. 2005; Nir et al. 2006). Moreover, in a real single-molecule fluorescence experiment, the bursts do not have a fixed size, but rather a distribution of sizes. Because it is difficult to predict such a distribution, the binomial calculation of the shot noise is performed using the empirical burst size distribution. Estimation of the FRET histogram width and shape, and subsequent comparison to the experimental histogram, recovers additional contributions to the FRET histogram width and shape and is necessary to extract the correct *D*–*A* distance distribution.

Bleaching and Blinking

Because of photophysical or photochemical reactions, a fluorophore may reach permanent (bleaching) or temporary (blinking) nonemitting states (Kong et al. 2007). Figure 3 shows a simulated ALEX histogram of freely diffusing, doubly labeled molecules of $E = 0.5$. In the simulation, the acceptor stochastically bleaches or blinks (Fig. 3, left and middle) once every ~300 cycles of absorption/emission. When APBS is used to analyze bursts during which the acceptor is either bleached or in a temporary dark state, a decrease in the number of acceptor photons and an increase in the number of donor photons are detected. This results in a decrease in the mean *E* value and an increase in the mean *S* value. The exact value depends on the timing and timescale of the bleaching or blinking relative to the burst duration. Because bleaching and blinking are stochastic processes, they occur randomly during the diffusion through the confocal spot, leading to a "tail" of events in the 2D *E*–*S* histogram bridging the *D*–*A* subpopulation ($E = 0.5$ and $S = 0.5$) with the *D*-only-like subpopulation ($E = 0$ and $S = 1$). When DCBS is used (lower row), most of the events caused by blinking and bleaching are removed, leaving the histogram with the *D*–*A* subpopulation.

Random Coincidence of Diffusing Species

As discussed earlier, to achieve single-molecule resolution, the sample concentration is ≤100 pM. This ensures low probability of having two diffusing molecules in the confocal spot at the same time, because this random coincidence will alter the *E* and *S* values. If the concentration is >100 pM (Fig. 3, right; 300 pM), "bridges" between subpopulations are formed, altering the shape and the center of the distributions; DCBS minimizes such effects.

Detection and Excitation Volume Mismatch

Mismatch between the donor- and the acceptor-detection volumes broaden the FRET histogram. The mismatch between detection volumes simply means that the ratio between the probability of detecting a donor photon and the probability of detecting an acceptor photon depends on the location of the emitter. This can be owing to chromatic aberrations of the optics or to misalignment of the detectors or pinhole. The net result is that the ratio of donor- to acceptor-detected photons (and hence the *E* and *S*) depends on where the molecule is located in the confocal spot, leading to an additional spread of the measured *E* values.

µs-ALEX: Measuring Accurate FRET Efficiencies

Single-molecule FRET experiments that calculate proximity ratios are sufficient for studying the presence and relative abundance of various FRET states and subpopulations, as well as reporting on the kinetics of transitions between FRET states. However, it is often necessary to determine accurate FRET efficiencies and corresponding distances between fluorophores (e.g., in studies of protein translocation or determination of biomolecular structures). In these cases, it is necessary to perform corrections to remove photon cross talk and instrumental biases (Lee et al. 2005); such correction factors are available to all ALEX methods.

According to Förster theory, the accurate energy transfer efficiency E is related to the distance between the fluorophores by

$$E = \frac{R_0^6}{r^6 + R_0^6},$$

where R_0 represents the Förster radius of the pair of fluorophores used:

$$R_0^6 = \frac{9000(\ln 10)\kappa^2 Q_D}{128\pi^5 N n^4} \int_0^\infty F_D(\lambda)\varepsilon_A(\lambda)\lambda^4 d\lambda,$$

with $\kappa^2 = (\cos\theta_T - 3\cos\theta_D \cos\theta A)^2$.

The Förster radius is specifically related to the donor and acceptor fluorophore and can be determined out of experimental values, including the quantum yield of the donor Q_D, the fluorescence spectrum of the donor F_D, the wavelength-dependent extinction coefficient of the acceptor ε_A, the refractive index of the medium n, and Avogadro's number N. The relative orientation of the dye is expressed by κ^2, derived from the angle between the dipole moment of the donor and acceptor with respect to the connecting line (θ_D and θ_A) and relative to each other (θ_T). In case of freely rotating fluorophores, κ^2 can be approximated to 2/3.

CONCLUSION AND FUTURE PROSPECTS

Only a handful of biophysical approaches can be used to directly measure conformational changes, among them nuclear magnetic resonance (NMR) and small angle X-ray scattering (SAXS). These ensemble approaches will often be more informative but necessitate homogeneous and synchronizable conformational changes for proteins at concentrations in the micromolar range. In contrast, smFRET/ALEX permits study of small conformational changes that occur in a subpopulation of measured molecules without the need for synchronization and at picomolar concentrations. The caveat of note, however, is that a FRET only measures a single point-to-point distance that requires time-consuming sample preparation and is susceptible to error owing to changes in dye environment or other unexplained dye-related photophysics.

Nonetheless, smFRET with ALEX brings a new tool to the repertoire of structural biologists with which to probe Angstrom-level structural changes in biomolecules. This has thus far been most successfully applied to nucleic acid–based systems, such as polymerases, helicases, and ribosomes. These systems offer the practical advantage of facile and specific fluorophore labeling, whereas to study structural biology of protein system relies on less robust labeling strategies; nonetheless, several groups have investigated structural changes in protein folding and protein conformational dynamics without issue.

The use of smFRET/ALEX has become increasingly practical over the past 10 years owing to improvements in (1) the brightness of fluorescent dyes, (2) the availability of new and orthogonal biomolecule labeling chemistries, (3) the cost and availability of increasingly higher-precision optical elements, and (4) the cost and availability of lasers spanning the visible spectrum.

Cite this introduction as *Cold Spring Harb Protoc;* doi:10.1101/pdb.top086405

Advances in each of these domains will continue, contributing to the overall ease of the approach. Furthermore, groups will be able to probe the more intractable structural questions that require complex biochemical environments by performing smFRET/ALEX inside of cells. With advances in detector technology comes the prospect of multiple-confocal spot excitation and detection, allowing for high-throughput FRET measurements. Finally, the growing commercialization of the technology (by companies such as PicoQuant GmBH) enables one to envision facile smFRET/ALEX measurements at the push of a button by a biologist, akin to a fluorimeter.

REFERENCES

Deniz AA, Dahan M, Grunwell JR, Ha T, Faulhaber AE, Chemla DS, Weiss S, Schultz PG. 1999. Single-pair fluorescence resonance energy transfer on freely diffusing molecules: Observation of Förster distance dependence and subpopulations. *Proc Natl Acad Sci* **96:** 3670–3675.

Eggeling C, Berger S, Brand L, Fries JR, Schaffer J, Volkmer A, Seidel CA. 2001. Data registration and selective single-molecule analysis using multi-parameter fluorescence detection. *J Biotechnol* **86:** 163–180.

Ha T. 2001. Single-molecule fluorescence resonance energy transfer. *Methods* **25:** 78–86.

Ha T. 2004. Structural dynamics and processing of nucleic acids revealed by single-molecule spectroscopy. *Biochemistry* **43:** 4055–4063.

Ha T, Enderle T, Ogletree DF, Chemla DS, Selvin PR, Weiss S. 1996. Probing the interaction between two single molecules: Fluorescence resonance energy transfer between a single donor and a single acceptor. *Proc Natl Acad Sci* **93:** 6264–6268.

Hamadani KM, Weiss S. 2008. Nonequilibrium single molecule protein folding in a coaxial mixer. *Biophys J* **95:** 352–365.

Jager M, Michalet X, Weiss S. 2005. Protein–protein interactions as a tool for site-specific labeling of proteins. *Protein Sci* **14:** 2059–2068.

Jager M, Nir E, Weiss S. 2006. Site-specific labeling of proteins for single-molecule FRET by combining chemical and enzymatic modification. *Protein Sci* **15:** 640–646.

Kapanidis A, Majumdar D, Heilemann M, Nir E, Weiss S. 2015a. Assembling the μs-ALEX setup. *Cold Spring Harb Protoc* doi: 10.1101/pdb.prot086413.

Kapanidis A, Majumdar D, Heilemann M, Nir E, Weiss S. 2015b. Aligning the μs-ALEX setup. *Cold Spring Harb Protoc* doi: 10.1101/pdb.prot086421.

Kapanidis A, Majumdar D, Heilemann M, Nir E, Weiss S. 2015c. Sample preparation and data acquisition for μs-ALEX. *Cold Spring Harb Protoc* doi: 10.1101/pdb.prot086439.

Kapanidis AN, Weiss S. 2002. Fluorescent probes and bioconjugation chemistries for single-molecule fluorescence analysis of biomolecules. *J Chem Phys* **117:** 10953–10964.

Kapanidis AN, Lee NK, Laurence TA, Doose S, Margeat E, Weiss S. 2004. Fluorescence-aided molecule sorting: Analysis of structure and interactions by alternating-laser excitation of single molecules. *Proc Natl Acad Sci* **101:** 8936–8941.

Kapanidis AN, Laurence TA, Lee NK, Margeat E, Kong X, Weiss S. 2005a. Alternating-laser excitation of single molecules. *Acc Chem Res* **38:** 523–533.

Kapanidis AN, Margeat E, Laurence TA, Doose S, Ho SO, Mukhopadhyay J, Kortkhonjia E, Mekler V, Ebright RH, Weiss S. 2005b. Retention of transcription initiation factor σ^{70} in transcription elongation: Single-molecule analysis. *Mol Cell* **20:** 347–356.

Kapanidis AN, Margeat E, Ho SO, Kortkhonjia E, Weiss S, Ebright RH. 2006. Initial transcription by RNA polymerase proceeds through a DNA-scrunching mechanism. *Science* **314:** 1144–1147.

Kong X, Nir E, Hamadani K, Weiss S. 2007. Photobleaching pathways in single-molecule FRET experiments. *J Am Chem Soc* **129:** 4643–4654.

Laurence TA, Kong XX, Jager M, Weiss S. 2005. Probing structural heterogeneities and fluctuations of nucleic acids and denatured proteins. *Proc Natl Acad Sci* **102:** 17348–17353.

Lee NK, Kapanidis AN, Wang Y, Michalet X, Mukhopadhyay J, Ebright RH, Weiss S. 2005. Accurate FRET measurements within single diffusing biomolecules using alternating-laser excitation. *Biophys J* **88:** 2939–2953.

Margeat E, Kapanidis AN, Tinnefeld P, Wang Y, Mukhopadhyay J, Ebright RH, Weiss S. 2006. Direct observation of abortive initiation and promoter escape within single immobilized transcription complexes. *Biophys J* **90:** 1419–1431.

Nir E, Michalet X, Hamadani KM, Laurence TA, Neuhauser D, Kovchegov Y, Weiss S. 2006. Shot-noise limited single-molecule FRET histograms: Comparison between theory and experiments. *J Phys Chem B* **110:** 22103–22124.

Ross J, Buschkamp P, Fetting D, Donnermeyer A, Roth C, Tinnefeld P. 2007. Multicolor single-molecule spectroscopy with alternating laser excitation for the investigation of interactions and dynamics. *J Phys Chem B* **111:** 321–326.

Alternating Laser Excitation for Solution-Based Single-Molecule FRET

Achillefs Kapanidis, Devdoot Majumdar, Mike Heilemann, Eyal Nir and Shimon Weiss

Cold Spring Harb Protoc; doi: 10.1101/pdb.top086405